Enzymology:

Role of Ser-257 in the Sliding Mechanism of NADP(H) in the Reaction Catalyzed by the *Aspergillus fumigatus* Flavin-dependent Ornithine N^5-Monooxygenase SidA

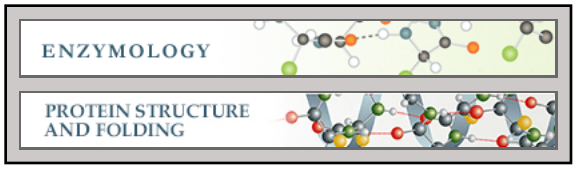

Carolyn Shirey, Somayesadat Badieyan and Pablo Sobrado

J. Biol. Chem. 2013, 288:32440-32448.
doi: 10.1074/jbc.M113.487181 originally published online September 26, 2013

THE JOURNAL OF BIOLOGICAL CHEMISTRY VOL. 288, NO. 45, pp. 32440–32448, November 8, 2013

Role of Ser-257 in the Sliding Mechanism of NADP(H) in the Reaction Catalyzed by the *Aspergillus fumigatus* Flavin-dependent Ornithine N^5-Monooxygenase SidA*

Received for publication, May 22, 2013, and in revised form, September 20, 2013 Published, JBC Papers in Press, September 26, 2013, DOI 10.1074/jbc.M113.487181

Carolyn Shirey[‡], **Somayesadat Badieyan**[‡], **and Pablo Sobrado**[‡§1]

From the [‡]*Department of Biochemistry and the* [§]*Virginia Tech Center for Drug Discovery, Virginia Tech, Blacksburg, Virginia 24061*

Background: SidA is a flavin-dependent monooxygenase that catalyzes the hydroxylation of ornithine and is essential for virulence in *Aspergillus fumigatus*.
Results: Mutation of Ser-257 leads to destabilization of the C4a-hydroperoxyflavin and a faster hydride transfer step.
Conclusion: Ser-257 is important for positioning $NADP^+$ in the correct orientation for stabilization of the C4a-hydroperoxyflavin.
Significance: The results support a sliding mechanism for NADP(H) in SidA.

SidA (siderophore A) is a flavin-dependent *N*-hydroxylating monooxygenase that is essential for virulence in *Aspergillus fumigatus*. SidA catalyzes the NADPH- and oxygen-dependent formation of N^5-hydroxyornithine. In this reaction, NADPH reduces the flavin, and the resulting $NADP^+$ is the last product to be released. The presence of $NADP^+$ is essential for activity, as it is required for stabilization of the C4a-hydroperoxyflavin, which is the hydroxylating species. As part of our efforts to determine the molecular details of the role of NADP(H) in catalysis, we targeted Ser-257 for site-directed mutagenesis and performed extensive characterization of the S257A enzyme. Using a combination of steady-state and stopped-flow kinetic experiments, substrate analogs, and primary kinetic isotope effects, we show that the interaction between Ser-257 and NADP(H) is essential for stabilization of the C4a-hydroperoxyflavin. Molecular dynamics simulation results suggest that Ser-257 functions as a pivot point, allowing the nicotinamide of $NADP^+$ to slide into position for stabilization of the C4a-hydroperoxyflavin.

Class B flavin-dependent monooxygenases are a family of enzymes that catalyze NADPH- and oxygen-dependent hydroxylation, epoxidation, and ester bond formation on a variety of substrates (1, 2). Members of this family of enzymes include the Baeyer-Villiger monooxygenases, flavin monooxygenases (FMOs),[2] and the *N*-hydroxylating monooxygenases. These enzymes have been studied for their application in the chemical industry and as potential drug targets (1, 3, 4). Our group has been interested in the structure and mechanism of action of *Aspergillus fumigatus* SidA (siderophore A), an *N*-hydroxylating monooxygenase involved in siderophore biosynthesis (5, 6). SidA catalyzes the hydroxylation of ornithine at the N^5-position (Scheme 1). This reaction is essential for the production of functional hydroxamate-containing siderophores in *Aspergillus* spp. Deletion of the *sidA* gene in *A. fumigatus* leads to a mutant strain that is avirulent in mouse models (7, 8). The absence of a SidA homolog in humans and the essential role of this enzyme in virulence suggest that SidA is an ideal drug target.

The mechanism of flavin-dependent monooxygenases can be divided into two half-reactions: the reductive half-reaction, in which the flavin cofactor is reduced by NADPH, and the oxidative half-reaction, in which the reduced flavin activates molecular oxygen, forming a covalent C4a-hydroperoxyflavin intermediate (Scheme 1). Stabilization of the oxygenated flavin intermediate is key to monooxygenation reactions (1, 9).

In recent years, the mechanism of stabilization of flavin intermediates in Class B flavin-dependent monooxygenases has been studied in significant detail. It was shown that $NADP^+$ plays a role in stabilization of the C4a-(hydro)peroxyflavin and that it remains bound throughout the catalytic cycle (10–13). Recently, our group reported the three-dimensional structure of *A. fumigatus* SidA (6). This is the first structure of a eukaryotic *N*-hydroxylating monooxygenase in complex with both $NADP^+$ and the hydroxylatable substrate ornithine. The structure clearly shows that the binding of $NADP^+$ is not optimal for hydride transfer but, instead, for its role in the stabilization of the C4a-hydroperoxyflavin (Fig. 1) (6). The position of $NADP^+$ suggests that it undergoes conformational changes after the hydride transfer step. This has been termed the sliding mechanism of NADP(H) in this family of enzymes (14, 15). In the active site of SidA, Ser-257 hydrogen bonds to the pyrophosphate of NADP(H) (Fig. 1). Here, we present biochemical data showing that Ser-257 plays an important role in the sliding mechanism of $NADP^+$ by acting as the pivot point, allowing the nicotinamide ring to slide into the position essential for stabilization of the C4a-hydroperoxyflavin.

EXPERIMENTAL PROCEDURES

Materials—Escherichia coli TOP10 and BL21(DE3)-T1[R] chemically competent cells were from Invitrogen. Plasmid pET15b was obtained from Novagen. DNA sequencing was performed at the Virginia Bioinformatics Institute DNA

* This work was supported in part by National Science Foundation Grant MCB 1021384 and by the Virginia Tech Biodesign and Bioprocessing Center.
[1] To whom correspondence should be addressed: Dept. of Biochemistry, Virginia Tech, Blacksburg, VA 24061. Tel.: 540-231-9485; Fax: 540-231-9070; E-mail: psobrado@vt.edu.
[2] The abbreviations used are: FMO, flavin monooxygenase; APADPH, 3-acetylpyridine-adenine dinucleotide phosphate; MD, molecular dynamics.

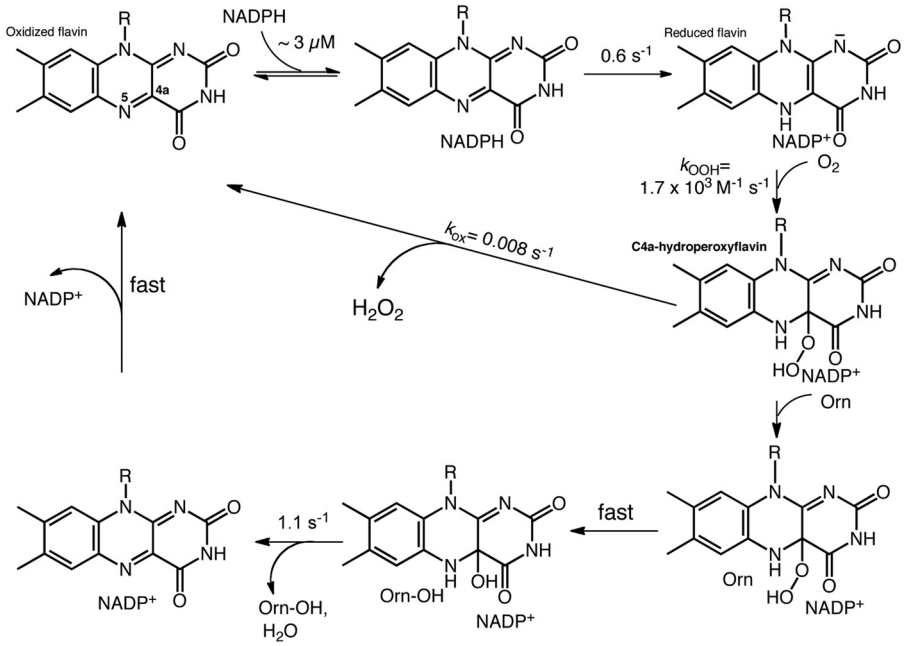

SCHEME 1. **The catalytic cycle of SidA.** In this reaction, $NADP^+$ plays an important role in the stabilization of the hydroxylating species, the C4a-hydroperoxyflavin. *Orn*, ornithine.

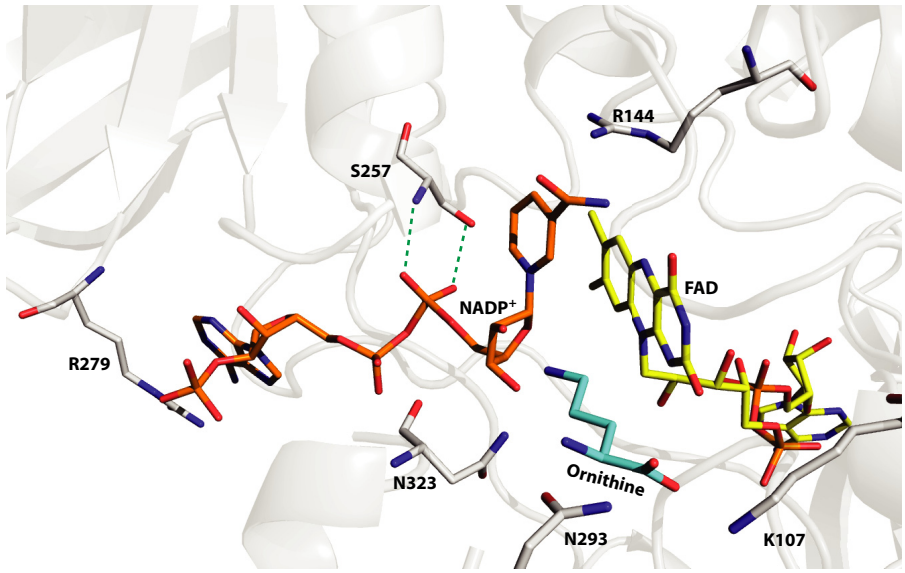

FIGURE 1. **Active site of SidA.** Residues predicted to interact with $NADP^+$ and ornithine are shown. The interaction of Ser-257 with the pyrophosphate group of $NADP^+$ is shown with a *dashed green line*. The figure was made using PyMOL and the coordinates of Protein Data Bank entry 4B63.

sequencing facility. Purification was performed on an ÄKTA Prime FPLC system (GE Healthcare). L-Ornithine, NADPH, NADH, buffers, and salts were purchased from Thermo Fisher Scientific and used without further purification. Reduced 3-acetylpyridine-adenine dinucleotide phosphate (APADPH) was purchased from MyBioSource.

Site-directed Mutagenesis—Site-directed mutagenesis reactions were performed using the QuikChange mutagenesis kit (Agilent Technologies, Santa Clara, CA) following the instructions provided by the manufacturer and using forward primer 5′-CTG GGC TCC GGC CAG GCC GCC GCC G-3′ and reverse primer 5′-CGG CGG CGG CCT GGC CGG AGC CCA G-3′. Primers were obtained from Integrated DNA Technologies (Coralville, IA).

Protein Expression and Purification—The genes coding for wild-type SidA and S257A enzymes were present in pET15b and transformed into *E. coli* BL21(DE3)-T1^R cells. The procedures for expression and purification of the recombinant proteins were essentially as previously described (6, 16).

Steady-state Kinetic Analyses—The amount of oxygen consumed was measured in a continuous assay using an oxygen measuring system from Hansatech Instruments Ltd. (Norfolk, England). The reaction mixture contained either NADPH (0.005–0.3 mM) or APADPH (0.05–2.0 mM) and saturating levels of L-ornithine (10 mM). The total volume was 1 ml of 100 mM sodium phosphate buffer (pH 7.5) at 25 °C. The reaction was initiated by the addition of 2 μM enzyme and monitored for 1 min with constant stirring. The iodine oxidation assay was per-

formed as described previously (5, 6, 17) to measure the amount of hydroxylated ornithine produced. The standard buffer for the iodine oxidation assay was 100 mM sodium phosphate buffer (pH 7.5). To determine the rate dependence on L-ornithine concentration, NADPH was held constant at 1 mM, and L-ornithine was varied (0–12 mM). The reaction contained 2 μM enzyme in a total volume of 104 μl at 25 °C.

Rapid Reaction Kinetics—The reductive half-reaction was monitored using an Applied Photophysics SX20 stopped-flow spectrophotometer placed inside a glove box. Anaerobic buffer was prepared by cycles of vacuum (20 min) and flushing oxygen-free argon (1 min) for 2 h. The enzyme was degassed by applying vacuum until bubbles were visible and then flushing with argon for 20 s. This procedure was repeated 10 times. Equal volumes of anaerobic enzyme at 30 μM were mixed with NADH and NADPH at 10–4000 and 5–800 μM, respectively (before mixing). Spectra were recorded using a photodiode array in a logarithmic scale until full reduction was achieved. The oxidative half-reaction was monitored using double mixing settings. Oxygen-saturated 100 mM sodium phosphate buffer (pH 7.5) was prepared by bubbling with 100% oxygen for 1 h with constant stirring. Varying O_2 concentrations ranging from 100 to 570 μM (after mixing) were prepared by mixing 100% oxygen-saturated buffer with anaerobic buffer. Equal volumes of 60 μM enzyme and NADPH were mixed to completely reduce the enzyme (10 s for S257A and 60 s for wild-type SidA) before mixing with O_2-saturated buffer. The final concentration of enzyme and NAD(P)H was 15 μM. The temperature was kept constant at 15 °C.

Synthesis of Deuterated Coenzymes—4-Pro-*R*-[^{2}H]NADPH was synthesized by the method of Jeong and Gready (18) with some modifications. Briefly, 25 mg of $NADP^+$ (5.6 mM final concentration), 480 μl of 2-propanol d_8 (1 M final concentration), and 50 units of alcohol dehydrogenase (*Thermoanaerobium brockii*) were added to 6 ml of 25 mM Tris-Cl (pH 9.0). The reaction was allowed to proceed for 30 min at 40 °C with light agitation until the A_{260}/A_{340} ratio reached a value of ~2.5. The reactions were filtered with an M_r 5000 cutoff filter (Amicon). The samples were then concentrated by rotary evaporation to ~1 ml, diluted 1:12 with ethanol, vortexed, and placed at −20 °C for 30 min. The precipitated samples were separated from the supernatant by centrifugation at 14,100 × *g* for 20 min at 4 °C. The resulting pellets were allowed to dry under a fume hood for 1 h to remove any residual ethanol. The samples were then resuspended in 250 μl of 25 mM Tris-Cl (pH 9.0) and stored at −20 °C.

Data Analysis—In the oxygen consumption assay, the initial rates were measured directly using the Oxygraph Plus program (Hansatech Instruments Ltd.). The initial rates in the iodine oxidation assay were determined by calculating the total hydroxylated ornithine produced using a hydroxylamine standard curve. The steady-state kinetic parameters were obtained by fitting the initial rates to the Michaelis-Menten equation using the program KaleidaGraph. The decrease in absorbance at 452 nm was fit to Equation 1.

$$A_t = c + a_1 e^{-(k_1 \cdot t)} + a_2 e^{-(k_2 \cdot t)} \quad \text{(Eq. 1)}$$

In this double exponential equation, *a* is the amplitude, *k* is the apparent rate constant for flavin reduction, and *c* is the final absorbance. The resulting k_1 values were plotted as a function of NADH concentration. The data from this analysis were fit to Equation 2 to obtain the rate constant for reduction (k_{red}) and the K_D value.

$$v = \frac{k_{red} \cdot [S]}{K_D + [S]} \quad \text{(Eq. 2)}$$

The k_{obs} for oxidation of S257A at 380 nm was determined by fitting the data to a single exponential equation and the oxidation at 452 nm to Equation 1. The k_{obs} for oxidation as a function of oxygen concentration was fit to a linear equation.

Molecular Dynamics (MD) Simulations—All simulations were performed using the GROMACS package (version 4.5.5) (19) with GROMOS96 53a6 force field parameters (20). The coordinates of oxidized wild-type SidA bound to $NADP^+$ were taken from Protein Data Base entry 4B63 (6), and the oxidized FAD topology parameters were taken from our previous work (21). The protonation states of ionizable residues were assigned based on pK_a values calculated using the H++ program (22). The protein was solvated in a box of single point charge (23) water molecules containing 100 mM NaCl with a minimum solute-box distance of 15 Å. The systems were energy-minimized using the steepest descent method, followed by two steps of equilibrations with position restraints of 1000 kJ/mol on all heavy protein atoms and crystal water molecules at 310 K as described previously (24). MD was then conducted in the absence of any restraints using the same constant particle, pressure, and temperature ensemble for at least 50 ns. Periodic boundary conditions were used for all simulations. The P-LINCS algorithm (19) was employed to constrain all of the covalent bond lengths. A 1.4-nm cutoff was applied for both the neighbor list and the short-range nonbonding interactions. Long-range electrostatic interactions were calculated by the smooth particle mesh Ewald method (25) using a Fourier grid spacing of 0.12 nm. The same conditions were applied for MD simulations of *in silico* SidA mutant S257A. Analyses were performed using utilities available in the GROMACS suite or by scripts written in-house.

RESULTS

Protein Expression—The S257A enzyme was expressed and purified following the procedures developed for the wild-type enzyme. Approximately 2.5 mg of enzyme was obtained per g of cell paste. The flavin content (60–70%) and the flavin spectra (data not shown) were similar for both mutant and wild-type enzymes.

Steady-state Kinetics—The activity of SidA, as measured by determining the amount of oxygen consumed or hydroxylated ornithine produced, is shown in Fig. 2, and the kinetic constants are summarized in Table 1. Following oxygen consumption, the K_m value of the S257A enzyme for NADPH was not significantly changed, whereas the k_{cat} value increased. In contrast, when the activity was determined by measuring the formation of N^5-hydroxyornithine, the k_{cat} value for the S257A enzyme was lower than that for the wild-type enzyme.

Deuterium Kinetic Isotope Effects—To determine whether substitution of Ser-257 has an effect on the hydride transfer

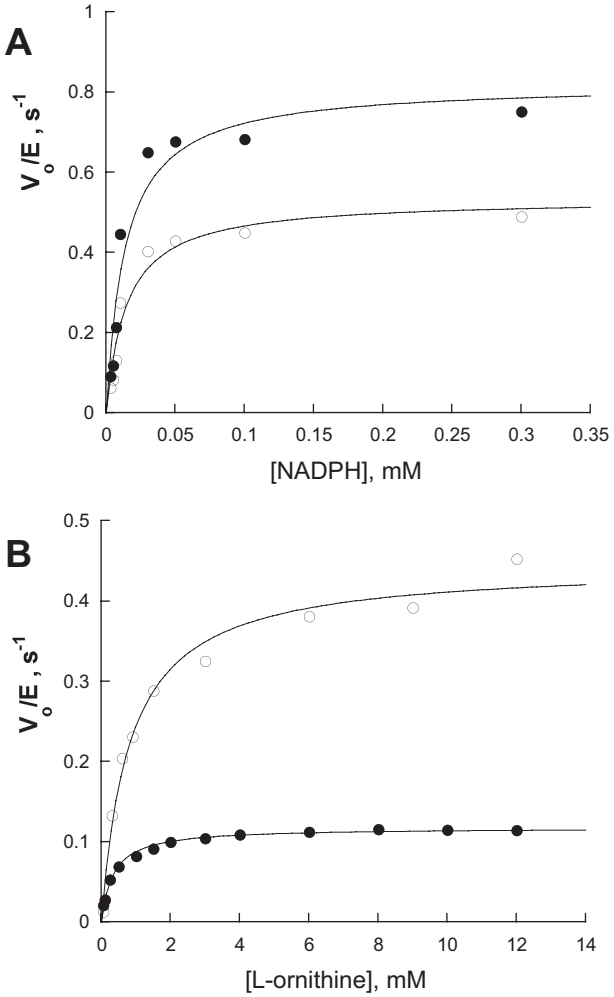

FIGURE 2. *A*, rate of oxygen consumption as a function of NADPH for wild-type SidA (○) and S257A (●). *B*, iodine oxidation assay to determine the rate of formation of hydroxylated ornithine as a function of L-ornithine for wild-type SidA (○) and S257A (●).

TABLE 1
Steady-state kinetic parameters
The buffer used was 100 mM sodium phosphate buffer (pH 7.5).

Parameter	Wild-type	S257A
O_2 consumption assay[a]		
k_{cat} (s^{-1})	0.60 ± 0.03	0.85 ± 0.01
$K_{m(NADPH)}$ (μM)	17 ± 3	14 ± 4
$k_{cat}/K_{m(NADPH)}$ (μM^{-1} s^{-1})	0.014 ± 0.004	0.04 ± 0.01
$^{D}k_{cat}$	3.1 ± 0.2	2.4 ± 0.1
Hydroxylamine detection assay[b]		
k_{cat} (s^{-1})	0.45 ± 0.02	0.12 ± 0.002
$K_{m(orn)}$ (mM)	0.80 ± 0.10	0.34 ± 0.03
$k_{cat}/K_{m(orn)}$ (mM^{-1} s^{-1})	0.54 ± 0.06	0.34 ± 0.03

[a] The concentration of ornithine was kept constant at 10 mM.
[b] The concentration of NADPH was kept constant at 1.0 mM.

step, the deuterium kinetic isotope effect on k_{cat} was measured (Table 1). We determined previously that the reaction is stereoselective for the transfer of the pro-*R*-hydrogen at C4 of NADPH to the oxidized flavin (16). Therefore, pro-*R*-[^{2}H]NADPH was used as the substrate, and the k_{cat} value was compared with the value obtained with NADPH. As determined previously for wild-type SidA (16), a $^{D}k_{cat}$ value of ~3.0 was observed, consistent with hydride transfer being partially rate-limiting. For the S257A enzyme, a $^{D}k_{cat}$ value of 2.4 was

TABLE 2
Presteady-state kinetic parameters
The buffer used was 100 mM sodium phosphate(pH 7.5).

Parameter	Wild-type	S257A
k_{red} (s^{-1})[a]	0.62 ± 0.01	2.50 ± 0.01
k_{red} (s^{-1})[b]	1.70 ± 0.02	5.54 ± 0.10
K_D (μM)[b]	56 ± 4	51 ± 4
k_{OOH} (M^{-1} s^{-1})	1.7×10^{3}[c]	2.5×10^{3}
k_{ox} (s^{-1})	0.008[c]	0.14
k_{ox} (M^{-1} s^{-1})		2.1×10^{3}

[a] Measured at 1.0 mM NADPH.
[b] Measured by varying the concentration of NADH (0.015–1.0 mM). SidA was reduced using stoichiometric concentrations of NADPH and mixed with varying concentrations of oxygen (0.1–0.5 mM) in the absence of ornithine.
[c] The data are taken from Ref. 29. k_{OOH} refers to the rate of formation of the C4a-hydroperoxyflavin, and k_{ox} refers to the rate of oxidation by elimination of the hydrogen peroxide (see Scheme 2).

measured. These results indicate that the mutation causes the hydride transfer step to be less rate-limiting. Further evidence for this is presented below.

Flavin Reduction—The k_{red} value was determined under anaerobic conditions as a function of NAD(P)H in a stopped-flow spectrophotometer (16, 26). The k_{red} value for the S257A enzyme was 4-fold higher than that for the wild-type enzyme (Table 2). However, the K_D value could not be accurately measured because the affinity appeared to be very high ($K_D \sim 1$ μM), similar to what was observed with the wild-type enzyme. The affinity for NADH was lower, and the K_D value was determined to be identical between wild-type SidA and S257A, whereas the k_{red} value was higher for the mutant enzyme (Table 2). Although consistent with the decrease in the primary kinetic isotope effect, the faster reduction rate is surprising, as replacement of Ser-257 was expected to have a negative impact on catalysis because potential hydrogen bonds with NAD(P)H are removed.

Flavin Oxidation—Oxidation of the reduced flavin can also be measured using a stopped-flow spectrophotometer. For SidA, it has been determined that in the absence of ornithine, a species with an absorbance maximum at 380 nm is observed (16, 26, 27). This species is very stable and corresponds to the C4a-hydroperoxyflavin, which slowly decays to yield oxidized flavin and hydrogen peroxide. The formation of oxidized flavin can be monitored by measuring the increase in absorbance at 452 nm. An example of the oxidation of wild-type SidA is shown in Fig. 3*A*. Here, the formation of the C4a-hydroperoxyflavin is clearly observed, and it decayed very slowly. When the same experiment was performed for the S257A enzyme, oxidation occurred without the formation of a stable C4a-hydroperoxyflavin. Dependence of the oxidation rate on oxygen concentration was also determined. For the wild-type enzyme, the rate constant for C4a-hydroperoxyflavin formation (k_{OOH}) was dependent on the concentration of oxygen. The rate constant for oxidation (k_{ox}) was very slow and was independent of the oxygen concentration (Table 2). For the S257A enzyme, oxidation at 380 nm was also dependent on the concentration of oxygen. In contrast, oxidation at 452 nm occurred in two phases in the S257A enzyme. One phase was concentration-dependent, and the rate constant was similar to the value determined at 380 nm (Table 2). The second phase was slow and did not change as a function of oxygen concentration (Fig. 3*C* and Table 2). The fast phase at 452 nm for S257A is consistent with

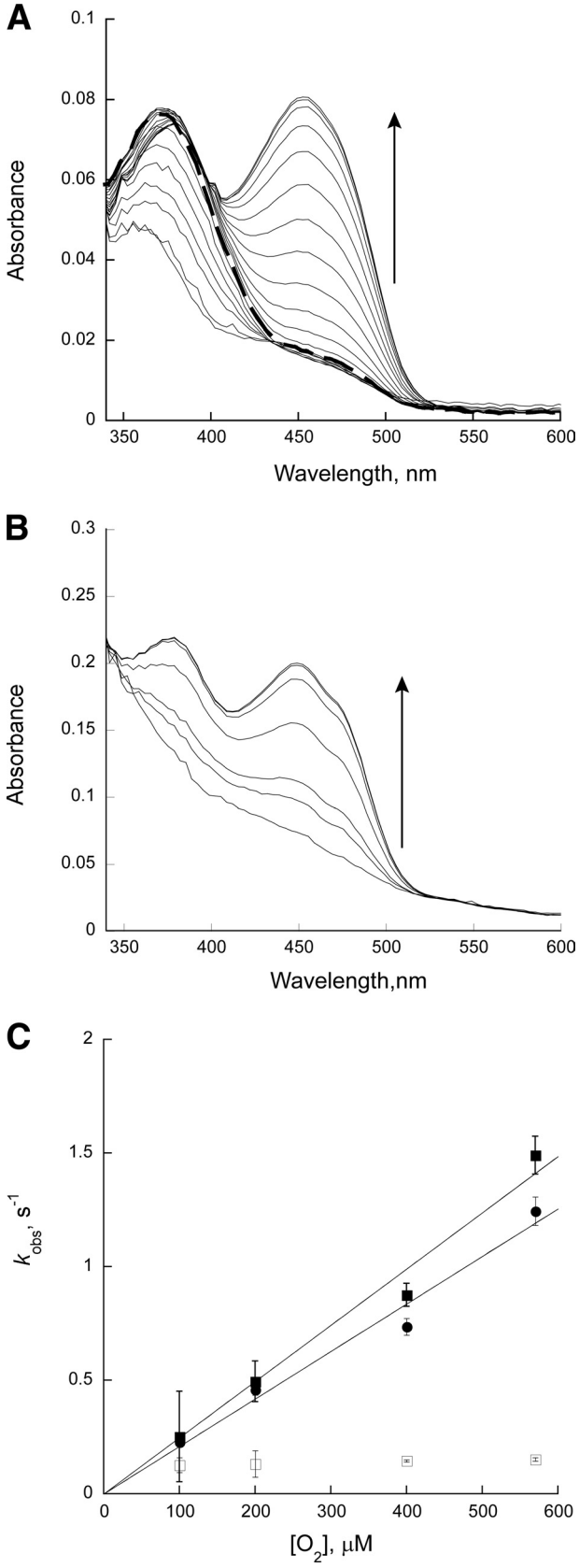

FIGURE 3. **Reaction of reduced flavin with oxygen in the absence of ornithine monitored in a stopped-flow spectrophotometer.** *A*, oxidation of wild-type SidA clearly shows the formation of an intermediate with a peak at 380 nm, which corresponds to the C4a-hydroperoxyflavin (*dashed line*). *B*, oxidation of Ser-257 does not show a peak at 380 nm, indicating that the C4a-hydroperoxyflavin is not stabilized. Full oxidation of the wild-type enzyme is achieved in >800 s, whereas for S257A, it is achieved in <60 s. *C*, oxidation of S257A as a function of oxygen concentration monitored at 380 nm (●) and 452 nm (■). The slow rate of oxidation at 452 nm that is independent of oxygen concentration is shown (□).

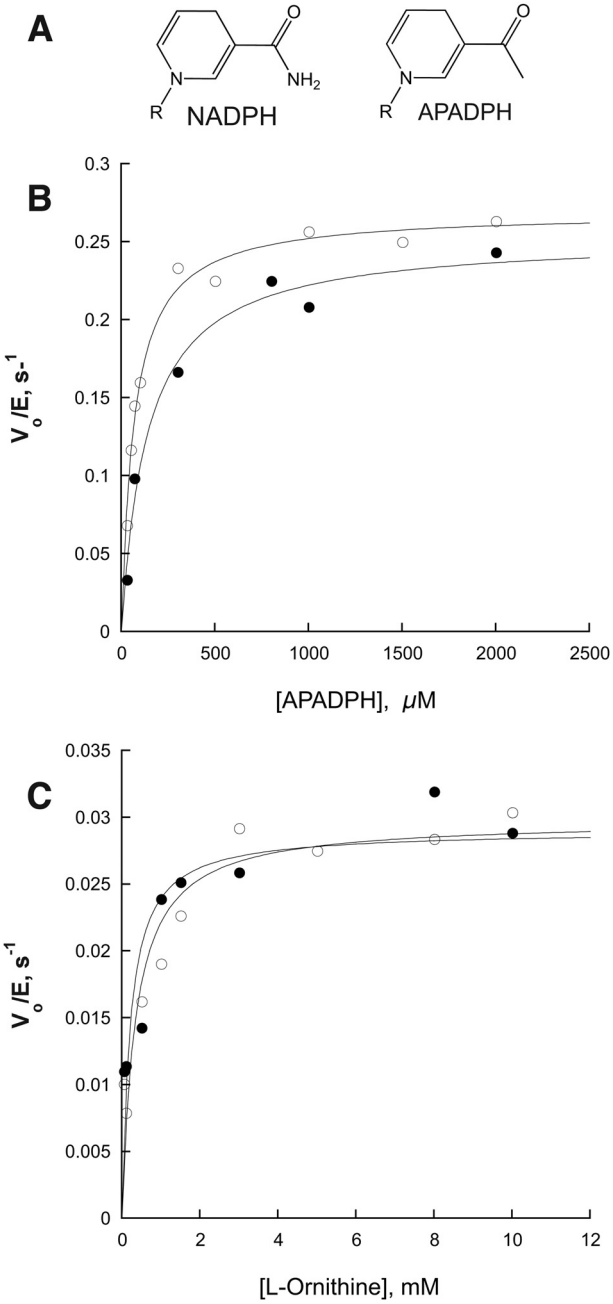

FIGURE 4. **Activity of wild-type SidA (●) and S257A (○) with APADPH.** *A*, structures showing differences between NADPH and APADPH. *B*, activity following the consumption of oxygen. *C*, activity determining the formation of hydroxylated ornithine. ●, SidA; ○, S257A.

the enzyme being unable to stabilize the C4a-hydroperoxyflavin intermediate. The slower phase at 452 nm is consistent with a small population of S257A that is able to stabilize this intermediate, which explains the 12% production of hydroxylated ornithine.

Activity with APADPH—APADPH is an analog of NADPH that lacks the amino moiety of the amide group (Fig. 4). Oxygen

TABLE 3
Steady-state kinetic parameters with reduced APADPH
The buffer used was 100 mM sodium phosphate buffer (pH 7.5).

Parameter	Wild-type	S257A
O_2 consumption assay[a]		
k_{cat} (s^{-1})	0.25 ± 0.01	0.27 ± 0.01
$K_{m(APADPH)}$ (μM)	140 ± 28	67 ± 6
$k_{cat}/K_{m(APADPH)}$ ($\mu M^{-1}\ s^{-1}$)	0.0018 ± 0.003	0.004 ± 0.0003
Hydroxylamine detection assay[b]		
k_{cat} (s^{-1})	0.03 ± 0.002	0.03 ± 0.002
$K_{m(orn)}$ (mM)	0.30 ± 0.10	0.21 ± 0.10
$k_{cat}/K_{m(orn)}$ ($mM^{-1}\ s^{-1}$)	0.14 ± 0.05	0.09 ± 0.03

[a] The concentration of ornithine was kept constant at 10 mM.
[b] The concentration of APADPH was kept constant at 1.0 mM.

consumption activity with APADPH was almost indistinguishable between the wild-type SidA and S257A enzymes (Fig. 4). Furthermore, a comparison of the hydroxylation activity showed that both enzymes displayed the same level of coupling (~12%) with this analog (Table 3).

MD Simulations—We carried out all-atom solvent-explicit MD simulations of wild-type SidA and S257A to characterize and track the dynamic behavior of the proteins, in particular, the dynamics of $NADP^+$. Ser-257 in wild-type SidA donates two hydrogen bonds (one through the amide nitrogen and the other through the hydroxyl group of the side chain) to oxygen atoms on the $NADP^+$ pyrophosphate group. Analyses of MD trajectories showed that hydrogen bond made by the amide nitrogen (~3.2 Å apart from the O1N atom of $NADP^+$) is unsteady and frequently breaks during the simulations, whereas the hydroxyl group establishes an almost stable hydrogen bond during simulations (~2.7 Å apart from the O2N atom of $NADP^+$). In the S257A enzyme, lack of the hydrogen bond between the side chain and $NADP^+$ makes the distance of Ala-257 and the pyrophosphate of $NADP^+$ highly fluctuating with an increasing trend (Fig. 5*A*). Further analyses indicated that the hydrogen bonds made by Ser-257 reduce the flexibility of $NADP^+$. Fig. 5*B* displays a considerable increase in root mean square deviation for the nicotinamide moiety of $NADP^+$ in S257A. In comparison, the nicotinamide ring is considerably more stable in wild-type SidA. The enhanced flexibility of the nicotinamide in the S257A enzyme results in C4 of the nicotinamide ring sampling shorter distances (<5.5 Å) to FAD N5 more frequently than observed in the wild-type enzyme (Fig. 5*C*). The higher flexibility of the nicotinamide ring and the sampling of shorter distances between NADP C4 and FAD N5 may facilitate the hydride transfer process in S257A.

The S257A mutation does not affect the overall protein flexibility, as both wild-type and mutant structures present the same backbone root mean square deviation. However, the average root mean square fluctuation per residue shows that the mutation changes some local fluctuation (data not shown). The differences are minor but consistent among replicates of simulations. The S257A mutation causes an increase in flexibility in two small loops, loop 253–257, which is within interacting distance of $NADP^+$ (including Ser-257 and Gln-256, which are able to form hydrogen bonds with $NADP^+$ during MD simulations), and loop 453–458, which resides 5 Å from the FAD phosphate group. In contrast, loop 97–105 (including Gln-102, which makes a hydrogen bond with FAD) presents reduced flexibility in the mutant enzyme.

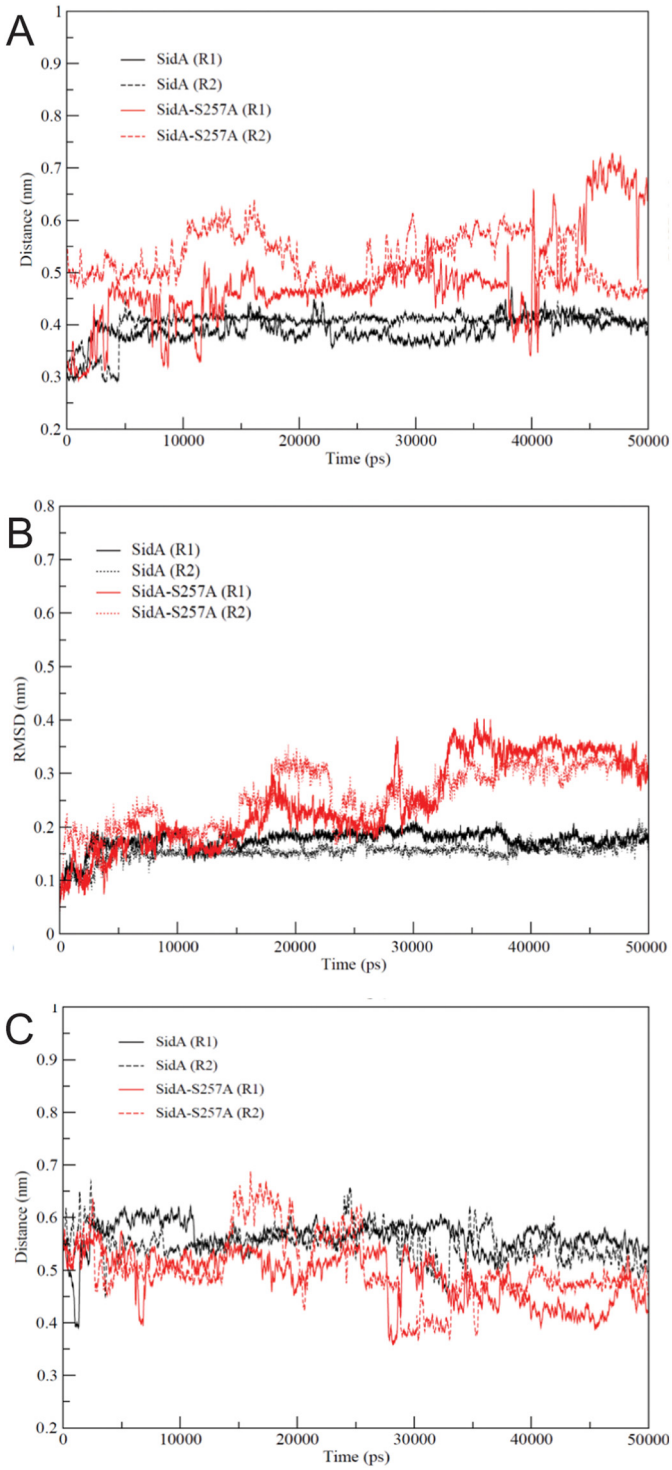

FIGURE 5. **MD simulation of wild-type SidA and S257A in complex with $NADP^+$.** *A*, average distance (in nm) of the side chain methyl group of Ser/Ala-257 to the center of the mass of the phosphate of $NADP^+$ (see Fig. 2). *B*, root mean square deviation (*RMSD*) of the nicotinamide ring of $NADP^+$ from the position observed in the crystal structure. *C*, average FAD N5-NADP C4 distance (in nm) during simulation. *R1* and *R2* indicate the replicates of each simulation.

DISCUSSION

Flavin-dependent monooxygenases catalyze the stereospecific insertion of an oxygen atom into a variety of substrates. A prerequisite for the oxygenation reaction is the reduction of the

flavin cofactor. This is necessary to activate molecular oxygen, which is accomplished via a single electron transfer from the reduced flavin, forming a reactive superoxide and a flavin semiquinone. This caged radical pair rapidly recombines to form a covalent flavin oxygen adduct at C4a of the flavin. Depending on the specific chemical outcome, a C4a-peroxyflavin or C4a-hydroperoxyflavin is formed (2, 9, 28). Formation of these intermediates does not ensure monooxygenation, as stabilization is required for optimal catalysis. If the intermediate is not stabilized, it rapidly decays to hydrogen peroxide and oxidized flavin, such as in the case of flavin oxidases (30). Thus, at the center of the activity of flavin-dependent monooxygenases is the stabilization of the C4a-(hydro)peroxyflavin intermediate.

SidA has been shown to function via a sequential kinetic mechanism, in which the enzyme first reacts with NADPH, followed by binding of ornithine and reaction with oxygen. In the absence of ornithine, reduced SidA forms a stable C4a-hydroperoxyflavin (~20-min half-life) (5, 26). The protein rapidly turns over only when ornithine is present, producing hydroxylated ornithine, $NADP^+$, and water. Stabilization of the C4a-hydroperoxyflavin ensures that the reaction is coupled, preventing the formation of hydrogen peroxide and futile consumption of NADPH. After reduction of the flavin, $NADP^+$ remains bound and is the last substrate to be released (5, 26). Reaction of chemically reduced SidA with oxygen and ornithine leads to 100% formation of hydrogen peroxide, highlighting the essential role of $NADP^+$ in the monooxygenation reaction of SidA. Thus, NADPH reduces the flavin, whereas $NADP^+$ plays an essential role in the stabilization of flavin intermediates in SidA. This dual or moonlighting role of NADP(H) has also been observed in the reaction of the related ornithine hydroxylase PvdA from *Pseudomonas aeruginosa* (31–33). A moonlighting role for NADP(H) was originally proposed for other members of the Class B flavin-dependent monooxygenases (12, 15, 34).

We recently solved the structure of SidA in both the oxidized and reduced forms and in complex with ornithine, lysine, or arginine (6). The structures show that $NADP^+$ binds in a conformation that forms a cavity that would allow the C4a-hydroperoxyflavin and the side chain amino group of ornithine to bind (Fig. 1). In addition, we also showed that reduction of the flavin results in interaction of the carbonyl oxygen of the amide group of $NADP^+$ with N5 of the flavin. This interaction is believed to be essential in preventing the release of hydrogen peroxide, as demonstrated in other flavin-dependent reactions (14, 29, 35, 36).

Here, we have shown that Ser-257 is essential for the role of $NADP^+$ in stabilizing the C4a-hydroperoxyflavin. Deletion of the hydrogen bond between the hydroxyl group of Ser-257 and the pyrophosphate of $NADP^+$ leads to interesting changes in the activity of SidA. When the rate of oxygen consumption was measured, the activity of the mutant enzyme was higher than that of the wild-type enzyme (Fig. 2). However, when formation of hydroxylated ornithine was measured, the activity of the mutant protein was shown to be much lower. The observed increase in oxygen consumption is due to an increase in uncoupling, presumably by production of hydrogen peroxide. In fact, it was determined that the S257A enzyme is only 12% coupled, whereas the wild-type enzyme has been determined to be 75–95% coupled (Table 1) (6). The increase in uncoupling suggests that the mutation affects the stabilization of the C4a-hydroperoxyflavin. This is supported by stopped-flow experiments that showed that a stable C4a-hydroperoxyflavin intermediate was not detected in the S257A enzyme under conditions in which, for the wild-type enzyme, the intermediate was stable for several minutes (Fig. 3).

To determine whether the affinity for NAD(P)H and the rate of hydride transfer were affected by the mutation, flavin reduction was monitored with a stopped-flow spectrophotometer. The affinity for NADPH appeared not to have been significantly affected because, even at the lower concentrations of NADPH that could be accurately tested (5 μM), the maximum rate of reduction was obtained. Similar to the wild-type enzyme, this indicates that the affinity for NADPH is in the low micromolar concentration (16, 26). The lack of effect on binding was also evident with NADH, where the K_D value could be measured in the stopped-flow instrument, and it clearly did not change in the mutant enzyme. Interestingly, the rate constant for flavin reduction was faster in the mutant enzyme (Table 2). The increase in the rate constant for flavin reduction is consistent with and provides an explanation for the observed decrease in the primary kinetic isotope determined with the Ser-257 enzyme (Table 1).

To gain further insight into the possible role of Ser-257, we tested the activity of the mutant enzyme with APADPH and compared it with that the wild-type enzyme. Upon monitoring the kinetics of oxygen consumption with this coenzyme, wild-type SidA displayed a k_{cat} value only ~2.4-fold lower than with NADPH, suggesting that APADPH is an effective redox partner for SidA. However, when the formation of hydroxylated ornithine was measured, it was determined that the reaction was only ~12% coupled (compared with 75–95% with NADPH). Interestingly, the kinetic parameters for the S257A enzyme are almost identical to those for wild-type SidA. Thus, the effect of the mutation is cancelled by the absence of the nitrogen in APADPH (Fig. 4*A*). Orru *et al.* (35) have reported the biochemical and structural characterization of bacterial FMO with APADPH. They concluded that this analog can effectively reduce the flavin of FMO and that the reaction is highly uncoupled (14), similar to the results shown here with SidA. Structural analysis of FMO in complex with $APADP^+$ showed that the ADP portion binds similarly to that of NADPH, but the pyrimidine ring is "flipped out," presumably due to the lack of interaction with flavin N5 and $APADP^+$. Thus, the analog does not bind in a conformation optimal for the stabilization of the oxygenated flavin intermediates. Similar effects were observed by mutating residues that interact with the amide group of the nicotinamide ring in FMO (35). Because NADP(H) is expected to play a similar role in SidA as reported for FMO, it is reasonable to assume that a similar effect occurs in SidA. In fact, the major effect when APADPH is used as a substrate is a significant uncoupling of the reaction, suggesting improper binding of the nicotinamide ring as shown for FMO. Interestingly, the S257A mutation affects mainly the stabilization of the C4a-hydroperoxyflavin, leading to high uncoupling. Thus, the mutation appears to affect the same step in the reaction.

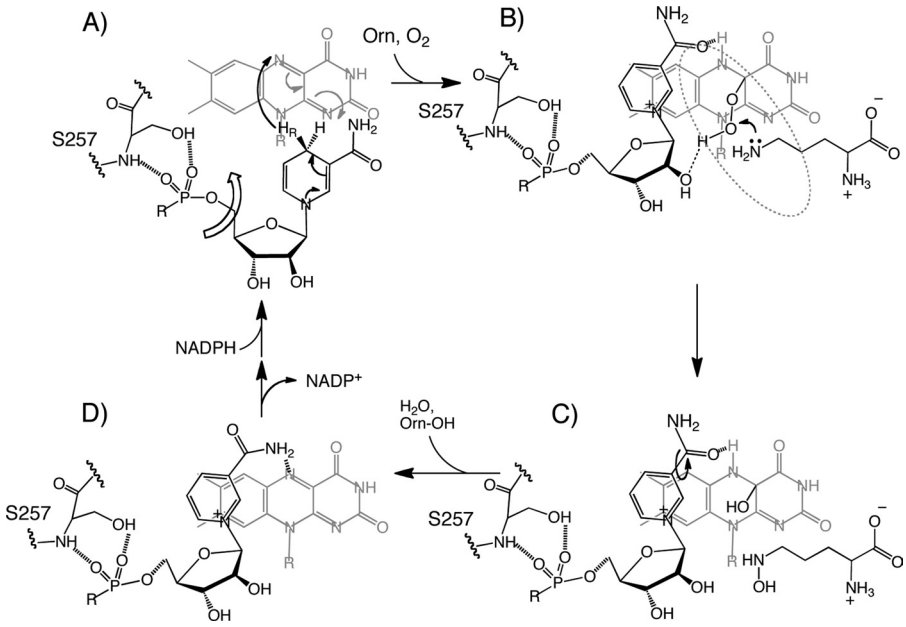

SCHEME 2. **Mechanism of stabilization of the C4a-hydroperoxyflavin in SidA.** *A*, the stereospecific hydride transfer by NADPH is the first step in the reaction. Note that the exact mode of binding of NADPH is not known. *B*, after hydride transfer, the nicotinamide ribose slide into a position that opens a cavity (*dotted lines*). Our results suggest that Ser-257 plays a key role in modulating this step. This cavity provides the space for the intermediate to form. The interaction between the amide carbonyl oxygen and flavin N5 provides key stabilizing interactions. In addition, hydrogen bonding between the distal oxygen of the intermediate and the 2′-ribose hydroxyl are predicted to occur. Furthermore, $NADP^+$ binding provides the space for ornithine N5-atom to be properly placed to attack the distal oxygen of the intermediate. *C*, the C4a-hydroxyflavin intermediate is dehydrated, and hydroxylated ornithine is released. *D*, $NADP^+$ is the last product to exit the active site. Oxidation of the flavin is accompanied by rotation of the amide bond of the nicotinamide ring of $NADP^+$, allowing the amino group to donate a hydrogen bond to flavin N5.

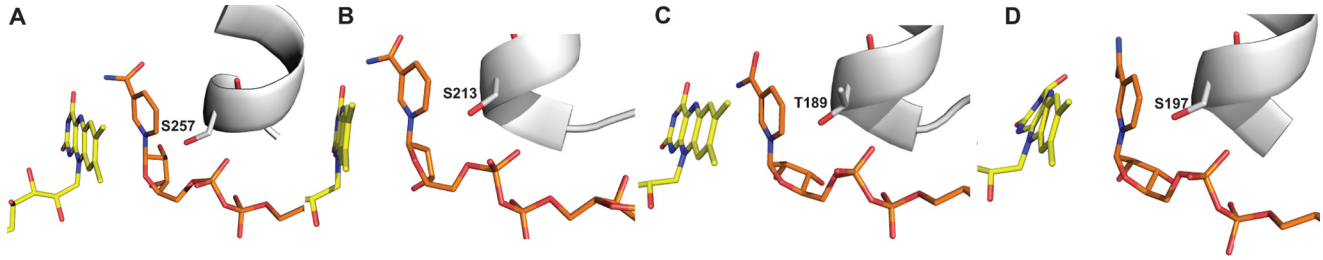

FIGURE 6. **The interaction between hydroxyl-containing residues and $NADP^+$ is conserved among members of the Class B FMOs.** *A*, SidA (Protein Data Bank entry 4B63). *B*, bacterial FMO (entry 2VQ7). *C*, cyclohexanone monooxygenase (entry 3GWD). *D*, phenylacetone monooxygenase (entry 2YLR).

The results from the MD simulations provide more direct clues to the role of Ser-257 in the reaction of SidA. The data show that in the absence of the hydrogen bond between the hydroxyl group of Ser-257 and $NADP^+$, the nicotinamide ring becomes more mobile (Fig. 5). These additional dynamics would prevent $NADP^+$ from binding in a conformation for the stabilization of the C4a-hydroperoxyflavin, but allowing the nicotinamide ring to sample closer interactions with the flavin. These results are consistent with the lack of stabilization of the C4a-hydroperoxyflavin and the higher rate of flavin reduction observed in the S257A enzyme.

Together, the data are consistent with the mechanism of stabilization of the C4a-hydroperoxyflavin by NADP(H) in SidA as shown in Scheme 2. We have shown previously that after hydride transfer, $NADP^+$ binds in a conformation important for stabilization of the C4a-hydroperoxyflavin. This positioning places the ribose 2′-hydroxyl group in hydrogen bonding distance to the distal oxygen of the C4a-hydroperoxyflavin. In addition, the carbonyl of $NADP^+$ is predicted to hydrogen bond with N5 of the intermediate. This interaction is essential for preventing the release of hydrogen peroxide. The cavity formed by $NADP^+$ is also important for substrate selectivity, as it provides the correct placement of the N^5-ornithine. It is clear that the position of NADPH during flavin reduction differs from the position of $NADP^+$ during the oxygenation reactions. Ser-257 plays an essential role in the mechanism that modulates the position of the coenzyme. In SidA, Ser-257 functions as the pivot point that allows the bond between the nicotinamide and the pyrophosphate to act as a hinge. This interaction is essential for the nicotinamide ring to slide into the position optimal for the oxygenation reaction. In the absence of this interaction, $NADP^+$ becomes more mobile and unable to acquire the correct position for optimal catalysis. A serine residue homologous to Ser-257 is conserved in all ornithine hydroxylases, including the prokaryotic PvdA (33, 37). In addition, a hydroxyl-containing amino acid is conserved in the same position of all known structures of Class B flavin-dependent monooxygenases (Fig. 6). It is possible that in this family of enzymes, hydroxyl-containing residues at this position function as the pivot point for NADPH to slide into position for stabilization of the C4a-(hydro)peroxyflavin.

REFERENCES

1. van Berkel, W. J., Kamerbeek, N. M., and Fraaije, M. W. (2006) Flavoprotein monooxygenases, a diverse class of oxidative biocatalysts. *J. Biotechnol.* **124,** 670–689
2. Massey, V. (1994) Activation of molecular oxygen by flavins and flavoproteins. *J. Biol. Chem.* **269,** 22459–22462
3. Torres Pazmiño, D. E., Winkler, M., Glieder, A., and Fraaije, M. W. (2010) Monooxygenases as biocatalysts: classification, mechanistic aspects and biotechnological applications. *J. Biotechnol.* **146,** 9–24
4. Ziegler, D. M. (2002) An overview of the mechanism, substrate specificities, and structure of FMOs. *Drug Metab. Rev.* **34,** 503–511
5. Chocklett, S. W., and Sobrado, P. (2010) *Aspergillus fumigatus* SidA is a highly specific ornithine hydroxylase with bound flavin cofactor. *Biochemistry* **49,** 6777–6783
6. Franceschini, S., Fedkenheuer, M., Vogelaar, N. J., Robinson, H. H., Sobrado, P., and Mattevi, A. (2012) Structural insight into the mechanism of oxygen activation and substrate selectivity of flavin-dependent *N*-hydroxylating monooxygenases. *Biochemistry* **51,** 7043–7045
7. Eisendle, M., Oberegger, H., Zadra, I., and Haas, H. (2003) The siderophore system is essential for viability of *Aspergillus nidulans*: functional analysis of two genes encoding L-ornithine N^5-monooxygenase (SidA) and a non-ribosomal peptide synthetase (SidC). *Mol. Microbiol.* **49,** 359–375
8. Hissen, A. H., Wan, A. N., Warwas, M. L., Pinto, L. J., and Moore, M. M. (2005) The *Aspergillus fumigatus* siderophore biosynthetic gene *sidA*, encoding L-ornithine N^5-oxygenase, is required for virulence. *Infect. Immun.* **73,** 5493–5503
9. Chaiyen, P., Fraaije, M. W., and Mattevi, A. (2012) The enigmatic reaction of flavins with oxygen. *Trends Biochem. Sci.* **37,** 373–380
10. Beaty, N. B., and Ballou, D. P. (1980) Transient kinetic study of liver microsomal FAD-containing monooxygenase. *J. Biol. Chem.* **255,** 3817–3819
11. Beaty, N. B., and Ballou, D. P. (1981) The oxidative half-reaction of liver microsomal FAD-containing monooxygenase. *J. Biol. Chem.* **256,** 4619–4625
12. Torres Pazmiño, D. E., Baas, B. J., Janssen, D. B., and Fraaije, M. W. (2008) Kinetic mechanism of phenylacetone monooxygenase from *Thermobifida fusca*. *Biochemistry* **47,** 4082–4093
13. Sheng, D., Ballou, D. P., and Massey, V. (2001) Mechanistic studies of cyclohexanone monooxygenase: chemical properties of intermediates involved in catalysis. *Biochemistry* **40,** 11156–11167
14. Orru, R., Dudek, H. M., Martinoli, C., Torres Pazmiño, D. E., Royant, A., Weik, M., Fraaije, M. W., and Mattevi, A. (2011) Snapshots of enzymatic Baeyer-Villiger catalysis. Oxygen activation and intermediate stabilization. *J. Biol. Chem.* **286,** 29284–29291
15. Mirza, I. A., Yachnin, B. J., Wang, S., Grosse, S., Bergeron, H., Imura, A., Iwaki, H., Hasegawa, Y., Lau, P. C., and Berghuis, A. M. (2009) Crystal structures of cyclohexanone monooxygenase reveal complex domain movements and a sliding cofactor. *J. Am. Chem. Soc.* **131,** 8848–8854
16. Romero, E., Fedkenheuer, M., Chocklett, S. W., Qi, J., Oppenheimer, M., and Sobrado, P. (2012) Dual role of NADP(H) in the reaction of a flavin dependent *N*-hydroxylating monooxygenase. *Biochim. Biophys. Acta* **1824,** 850–857
17. Robinson, R., and Sobrado, P. (2011) Substrate binding modulates the activity of *Mycobacterium smegmatis* G, a flavin-dependent monooxygenase involved in the biosynthesis of hydroxamate-containing siderophores. *Biochemistry* **50,** 8489–8496
18. Jeong, S. S., and Gready, J. E. (1994) A method of preparation and purification of (4*R*)-deuterated-reduced nicotinamide adenine dinucleotide phosphate. *Anal. Biochem.* **221,** 273–277
19. Hess, B. (2008) P-LINCS: a parallel linear constraint solver for molecular simulation. *J. Chem. Theory Comput.* **4,** 116–122
20. Oostenbrink, C., Villa, A., Mark, A. E., and van Gunsteren, W. F. (2004) A biomolecular force field based on the free enthalpy of hydration and solvation: the GROMOS force-field parameter sets 53A5 and 53A6. *J. Comput. Chem.* **25,** 1656–1676
21. Han, A., Robinson, R. M., Badieyan, S., Ellerbrock, J., and Sobrado, P. (2013) Tryptophan-47 in the active site of *Methylophaga* sp. strain SK1 flavin-monooxygenase is important for hydride transfer. *Arch. Biochem. Biophys.* **532,** 46–53
22. Anandakrishnan, R., Aguilar, B., and Onufriev, A. V. (2012) H++ 3.0: automating p*K* prediction and the preparation of biomolecular structures for atomistic molecular modeling and simulations. *Nucleic Acids Res.* **40,** W537–W541
23. Berendsen, H. J. C., Postma, J. P. M., van Gunsteren, W. F., DiNola, A., and Haak, J. R. (1984) Molecular dynamics with coupling to an external bath. *J. Chem. Phys.* **81,** 3684–3690
24. Badieyan, S., Bevan, D. R., and Zhang, C. (2012) A salt-bridge controlled by ligand binding modulates the hydrolysis reaction in a GH5 endoglucanase. *Protein Eng. Des. Sel.* **25,** 223–233
25. Darden, T., York, D., and Pedersen, L. (1993) Particle mesh Ewald: an *N*·log(*N*) method for Ewald sums in large systems. *J. Chem. Phys.* **98,** 10089–10092
26. Mayfield, J. A., Frederick, R. E., Streit, B. R., Wencewicz, T. A., Ballou, D. P., and DuBois, J. L. (2010) Comprehensive spectroscopic, steady state, and transient kinetic studies of a representative siderophore-associated flavin monooxygenase. *J. Biol. Chem.* **285,** 30375–30388
27. Romero, E., Robinson, R., and Sobrado, P. (2012) Monitoring the reductive and oxidative half-reactions of a flavin-dependent monooxygenase using stopped-flow spectrophotometry. *J. Vis. Exp.* **61,** e3803 doi: 10.3791/3803
28. Eppink, M. H., Boeren, S. A., Vervoort, J., and van Berkel, W. J. (1997) Purification and properties of 4-hydroxybenzoate 1-hydroxylase (decarboxylating), a novel flavin adenine dinucleotide-dependent monooxygenase from *Candida parapsilosis* CBS604. *J. Bacteriol.* **179,** 6680–6687
29. Romero, E., Avila, D., and Sobrado, P. (2013) in *Flavins and Flavoproteins* (Miller, S., Hille, R., and Palfey, B., eds) pp. 289–294, Lulu, Raleigh, NC
30. Mattevi, A. (2006) To be or not to be an oxidase: challenging the oxygen reactivity of flavoenzymes. *Trends Biochem. Sci.* **31,** 276–283
31. Meneely, K. M., Barr, E. W., Bollinger, J. M., Jr., and Lamb, A. L. (2009) Kinetic mechanism of ornithine hydroxylase (PvdA) from *Pseudomonas aeruginosa*: substrate triggering of O_2 addition but not flavin reduction. *Biochemistry* **48,** 4371–4376
32. Meneely, K. M., and Lamb, A. L. (2007) Biochemical characterization of a flavin adenine dinucleotide-dependent monooxygenase, ornithine hydroxylase from *Pseudomonas aeruginosa*, suggests a novel reaction mechanism. *Biochemistry* **46,** 11930–11937
33. Olucha, J., Meneely, K. M., Chilton, A. S., and Lamb, A. L. (2011) Two structures of an *N*-hydroxylating flavoprotein monooxygenase: ornithine hydroxylase from *Pseudomonas aeruginosa*. *J. Biol. Chem.* **286,** 31789–31798
34. Alfieri, A., Malito, E., Orru, R., Fraaije, M. W., and Mattevi, A. (2008) Revealing the moonlighting role of NADP in the structure of a flavin-containing monooxygenase. *Proc. Natl. Acad. Sci. U.S.A.* **105,** 6572–6577
35. Orru, R., Torres Pazmiño, D. E., Fraaije, M. W., and Mattevi, A. (2010) Joint functions of protein residues and NADP(H) in oxygen activation by flavin-containing monooxygenase. *J. Biol. Chem.* **285,** 35021–35028
36. Sucharitakul, J., Wongnate, T., and Chaiyen, P. (2011) Hydrogen peroxide elimination from C4a-hydroperoxyflavin in a flavoprotein oxidase occurs through a single proton transfer from flavin N5 to a peroxide leaving group. *J. Biol. Chem.* **286,** 16900–16909
37. Olucha, J., and Lamb, A. L. (2011) Mechanistic and structural studies of the *N*-hydroxylating flavoprotein monooxygenases. *Bioorg. Chem.* **39,** 171–177